



High-cycle fatigue behavior and chemical composition empirical relationship of low carbon three-sheet spot-welded joint: An application in automotive industry

K. Reza Kashyzadeh ^{a,*}, S. Ghorbani ^b

^a Department of Transport, Academy of Engineering, RUDN University, 6 Miklukho-Maklaya St., Moscow, 117198, Russian Federation.

^b Department of Mechanical Engineering Technologies, Academy of Engineering, RUDN University, 6 Miklukho-Maklaya St., Moscow, 117198, Russian Federation.

PAPER INFO

Paper history:

Received 01 May 2023

Received in revised form 07 June 2023

Accepted 08 June 2023

Keywords:

Resistance spot weld

Three-sheet welded joint

High-cycle fatigue

Chemical composition

Empirical relationship

In this paper, the authors have attempted to provide an empirical relationship between the fatigue behavior of three-sheet spot-welded joint and the chemical composition of low carbon steel. To this end, the application of this joint in the automotive industry was considered and laboratory samples were prepared based on the actual specifications in the industry, including the raw material (i.e., material and thickness of the primary sheets), the resistance spot welding (RSW) process parameters, and other factors. The results of tensile and quantitative tests along with microscopic observations were utilized to evaluate the raw material and to study the compliance of the steel grade with the required standards. Next, axial cyclic test was performed in order to extract the high-cycle fatigue (HCF) properties of three-sheet spot-welded joint. Finally, a relationship between the number of cycles to failure of the spot-welded joint, repetitive load level, and the percentage of constituent elements was presented by multiple linear regression (MLR) technique. The results showed that the greatest effect of the constituent elements is when we are in the regime of low-cycle fatigue (LCF) and by moving towards the HCF regime, its importance decreases until it becomes almost ineffective in the very-high-cycle fatigue (VHCF) area. In addition, the presented relationship is able to predict the fatigue behavior of three-sheet spot-welded joint via the chemical composition of the primary sheet and the cyclic force with a maximum error of 13.8% compared to the experimental results.

ABSTRACT

doi:

1. INTRODUCTION

Welding is one of the most common construction and repair techniques in large industries. There are various welding processes that must be chosen depending on the type of application, either construction or repair [1]. Also, in the construction of parts and assemblies by welding, it is necessary to take into account design considerations and determine the type of welding used based on different factors. For instance, in the automotive industry, RSW is used to manufacture body-in-white (BIW). It is reported that about 3000-5000 and in some documents up to 7000 spot welds are needed to make the BIW of a passenger car [2-5]. One of the main advantages of this type of welding compared to others is that there is no need for an electrode or intermediate material. In addition, the production speed and automation issue are very important. Therefore, a lot of research has been done in the field of spot welding. From the authors' viewpoint and based on their industrial experience, these studies are summarized in four different classifications. The first group is dedicated to the RSW process simulation. In this group,

different algorithms for simulating the process are presented as coupled analyses. In this regard, one of the most advanced and accurate algorithms includes the analysis of quadruple coupling, i.e., electrical-thermal-metallurgical-mechanical (ETMM). The superiority of this simulation algorithm provided by Reza Kashyzadeh et al. [6] is continuous software simulation with laboratory results. For this purpose, they used the results of various mechanical, material, and metallurgical experiments, including the initial phase and grain size of steel sheets, to define the material properties in the software. In addition, phase changes are also included in their model. Ueda et al. have applied incrementally coupled electrical-thermal-mechanical (ETM) simulation procedure in order to assess the spot welding with high accuracy [7]. They also considered the phase change and transformation. The authors claimed that using this method one can estimate the fatigue crack growth for any sheet assembly under any welding conditions with high accuracy. Sadeghian et al. have used finite element method (FEM) to study the nugget size and diffusion of metallic elements of the steels in the molten region during spot welding of 304 stainless steel to St37 carbon steel [8]. It is reported that

*Corresponding Author Email: reza-kashi-zade-ka@rudn.ru
(Prof. Dr. K. Reza Kashyzadeh)

the FEM has a high acceptance to predict the residual stress during welding [9] as well as its effects on microstructural defects and mechanical properties [10, 11]. Moreover, Garcia et al. have simulated the residual stress and deformation magnitude/distribution during the welding thermal cycle to determine the hardening rule [12]. In another work, Farrahi et al. have employed an ETM coupling of the 3D FEM to investigate the effects of different RSW process parameters (i.e., electric current, electrode force, up-slope, squeeze, welding time, and hold) on the nugget size and electrode penetration depth [13]. The authors stated that, as depth of electrode penetration raises, the deformation of the sheets also increases. It is also concluded that electric current and welding time, respectively, have the biggest impact on the nugget diameter. As it is clear from the results obtained in the first group, scholars seek to extract the geometric characteristics of the weld point, including the geometric shape (e.g., nugget size). Besides, the stress distribution contours at the welding point, sheet, and sometimes with the purpose of checking the electrode and its efficiency, temperature distribution has been seen in the electrode [14, 15]. Nevertheless, some researchers have been paid attention to the tension residual stress (TRS) profile resulting from the welding process in the sheets as well. Because such tension stresses are known as harmful stresses and lead to a decrease in the strength of the welded joint under static loads. Also, it results in vibration, dynamic behavior, and even cyclic load (fatigue phenomenon) [16–19]. Of course, it is rarely seen in simulations that both parts of the RSW process and fatigue analysis are performed simultaneously.

The second group of research is devoted to the optimization of the welding process with the aim of increasing the strength of the welded joint or producing a defect-free welded joint. In this group, scholars try to repeat the simulation of the RSW in different modes by changing the values of the process parameters and finally, according to the determined objective function, they are on the path of optimization. To increase the strength, researchers must consider a certain range for different parameters according to the equipment available or used in the industry (e.g., maximum electrode force of 1000 N). Also, to achieve this goal, they can use classic, modern, and other optimization's criteria. Moreover, some studies tried to utilize data mining and machine learning techniques, such as artificial neural networks (ANNs), backpropagation in neural networks, k-nearest neighbor, logistic regression and its regularized versions, random forest algorithms, auto-encoder classifiers, sequence tagging, support vector machine, tree-based machine learning methods, and speeded-up robust features method [16]. However, when the goal is to produce a defect-free spot-welded joint, the main focus is on strength defects like undersized weld and stick weld caused by suboptimal penetration depth. On the other hand, different relations provided in the standards, considering the application of the joint, can be used to choose the appropriate size of the spot weld core. For example, in the standards related to the RSW strength, there are several relationships between the nugget diameter of healthy weld and the thickness of the sheets (Equations 1 and 2).

$$D = 4\sqrt{t} \quad (1)$$

$$D = 4\sqrt[3]{t^2} \quad (2)$$

However, in the automotive industry, the following guidelines are used to determine the nugget diameter.

$$D = 4 \text{ mm} \quad 0.57 \text{ mm} < t_{min} < 1.27 \text{ mm}$$

Muthu has applied Taguchi approach (TA) and ANOVA to optimize the welding parameters (i.e., electrode diameter, heating time, and welding current, etc.) and study their effects on the quality characteristics of spot weld [21]. Maalouf et al. have introduced kernel ridge regression (KRR) method to study the influence of welding time, electrode force, and welding current on the nugget size and failure strength of the RSWs [22]. ANN approach has been applied to predict the weld penetration depth and weld bead width by Chokkalingham et al. [23]. Luo et al. have employed ANN approach and nonlinear multiple regression analysis (NMRA) to propose a mathematical model for predicting the nugget diameter and RSW strength of galvanized steel [24].

The third group of research deals with the evaluation of the quality of the spot weld. In other words, they try to identify defects caused by the welding process. Although advanced equipment is used in the industry for quality inspection, it is sometimes seen that the guidelines used in the industry are not in line with the achievements of researchers and they use the initial guidelines or updated by themselves. Sometimes it can be seen that the accuracy of scientific achievements is much higher because two parameters of time and cost are not defined for it compared to commercial works. Meanwhile, an industry should prioritize these two parameters for competitiveness. In this section, we can refer to destructive tests (DT) and non-destructive tests (NDT). In DTs, the sample is completely damaged and cannot be used again, usually they open the weld and measure the nugget diameter. But in NDTs, the welded joint is not damaged, and it can be used in the next steps. Among the most important methods are visual inspection, ultrasonic waves, X-Ray and gamma-ray radiography test, magnetic particle inspection, liquid penetrant test, eddy current test as NDTs [25], tensile test, bending test, impact test, hardness test, and etch test as DTs [26]. Ultrasonic inspection has shown itself to be an excellent method for quality control of spot welds due to minimizing human error, reliability in repeatability, evaluation, and interpretation of results [27]. Amiri et al. have combined ultrasonic testing method and ANN simulation to present a new methodology to estimate the static and fatigue behavior of three-sheet spot-welded joints [28]. Moreover, Ghafarallahi et al. have performed theoretical, numerical, and experimental studies to inspect the triple-layered spot-welded joints of low carbon steel sheets using ultrasonic waves [29]. Hua et al. have proposed a special in-situ ultrasonic detection system, which can calculate the nugget diameter and thickness, and classify the weld quality into good weld, over-burning weld, loose weld, thin-nugget weld, small-nugget weld, and internal-defect weld [30]. Moghanizadeh has employed ultrasonic test and design of experiment (based on Box-Behnken) to evaluate the quality and microhardness of the RSW in terms of attenuation coefficient of ultrasonic testing [31].

The last group analyzes the failure of welded joints. In addition to studying failure surface, they look for the root cause of failure. Most of the failures are due to material and metallurgical factors such as the formation of brittle phases, microstructural changes, and the creation of nano/microcracks [19, 32]. All possible factors must be investigated in the heat-

affected zone (HAZ). On the other hand, the prediction of HAZ softening is crucial in terms of controlling and optimizing the spot welds, since it has a strong impact on the failure mode and load-bearing capacity [33, 34]. Farrahi et al. have studied the failures of spot welds due to fatigue in a vehicle body [19]. It was concluded that the fatigue life of the spot welds is significantly affected by nugget diameter. Chen et al. have conducted tensile–shear tests to study the failure mode and mechanical properties of microscale RSWs [32]. The results revealed interfacial and pullout failure modes. It is also shown that the failure mode is mostly determined by the nugget size. Moreover, Pouranvari and Marashi have claimed that failure zone size, porosity, and shrinkage voids in the weld nugget as well as the hardness ratio of fusion zone to pull-out failure location are the key metallurgical factors influencing the failure mode of spot welds during the quasi-static tensile–shear test [35].

Despite the extensive research that has been done in this production method in various industries, as well as the development of non-destructive inspection and quality control technologies, and the introduction of advanced production technologies, we still see many failures in spot-welded joints. Thus, there is a gap in previous research that has been overlooked by researchers, yet has an impact on spot-welded joint strength. In this paper, an attempt has been made to investigate the effect of the chemical composition of the primary sheets (i.e., raw material) and in other words, the range of changes of the primary properties of the sheets to evaluate the fatigue strength of the three-sheet spot-welded joint with the purpose of application in the automotive industry. Because the authors believe, the initial controllers of the input stations of the primary sheets to the factories operate according to the defined standards, but even so, considering the control of all the same production conditions, the dispersion in the response of destructive and non-destructive tests is high. Consequently, as a hypothesis for the gap stated above, this issue was investigated.

2. METHODOLOGY

The main purpose of this article is to examine the hypothesis presented by the authors. In other words, they believe that the chemical composition of steel components, even to a small extent, can affect the quality of the RSW and subsequently the strength of the spot-welded joint under cyclic loading. For this purpose, a three-sheet single spot-welded joint was selected in the car body. This joint was not complicated because it contains one material and a certain thickness. The primary sheets were provided and subjected to different tensile, metallurgical (i.e., initial phase and grain size), and hardness tests in several different time steps. The results indicated that in some cases, the percentage of chemical compositions as well as the yield strength (YS) and ultimate tensile strength (UTS) of the sheets have changed. Although, all of them are within the permissible range declared by the internal or standard instructions or the key to steel reference, and this means that all of them can be used in the production line as one material.

However, the authors created different groups of primary sheets, each of which has nearly 100% identical material and mechanical properties. Then according to the parameters of the mentioned welding process to obtain a defect-free spot-welded joint based on the data of the car body manufacturer and using the fixture, which was previously designed and made by the

first author and his colleagues, the joints were made. It should be noted that in each joint, all three sheets were selected from the same group. After preparing the samples, axial fatigue test was performed, and the strength of the joints was obtained. Finally, by interpreting the results and using the non-linear multiple regression method, it was attempted to obtain an empirical relationship between the percentage of the constituent elements of sheets and the fatigue strength of the spot-welded joint. In this way, by knowing the percentage of the constituent elements of sheets and the applied cyclic force, the number of cycles required until failure can be obtained with proper accuracy.

3. EXPERIMENTAL PROCEDURE

In this research, a three-sheet spot-welded joint was considered in a non-critical part of the car body. Because in past studies, it has been determined that critical spot-welded joints in BIW consist of sheets with different materials and thicknesses. On the other hand, it is necessary to consider the simplest case for the initial study of a hypothesis and then study more difficult and acute conditions. Therefore, the authors initially classified spot-welded joints of BIW based on the type of sheets and thicknesses. Then, groups of joints that have the same sheet material and thickness are separated and the most critical one was studied. This joint consists of three sheets of 1.0347 mild low carbon steel with a thickness of 0.8 mm, produced by cold rolling method. To check the incoming sheets to the car factory, several sheets were randomly sampled from a certain supplier during a month. In this way, tensile test samples were prepared according to ASTM 8EM standard. Tensile test was done for 100 samples. In order to equalize the thickness of the tensile test sample on both sides, aluminum tabs with length, width, and thickness of 40, 45, and 0.8 mm were used. In this way, one tab was used on one side and two tabs were used on the other side, and finally the thickness of the sample was equal to 2.4 mm along the entire length. All tests were performed at ambient temperature and with a speed of moving the jaws equal to 8 mm/min. In addition, for each of the samples, a quantitative test was performed to extract the percentage of their chemical compositions. This test was done in IRAN test & research center for auto parts company (ITRAC). Also, metallographic tests were performed to detect the initial phase of the sheets and their grain size according to the instructions given in the ASM handbook volume 9. Moreover, microhardness test was performed to determine the hardness of the samples. Finally, the results showed that all the samples, in other words, all the sheets entering the factory, passed the stated standard for identifying the sheet type, 1.0347. Because all the obtained values were in the permissible range mentioned in the desired standard. For example, UTS for this steel is defined in the range of 270-370 MPa and the results obtained for all samples show that they are in this range. However, the results were scattered. Therefore, the authors divided the primary sheets into several different groups. In this way, the upper and lower limits of UTS were known according to the standard, and an interval of 10 MPa was considered for each group. After categorizing the results, it was found that four groups have the highest abundance. Therefore, the focus was on the data of these four groups. In each group, 60 sheets were prepared with the length and width of 125 mm and 45 mm, respectively. Then by using the fixture pre-designed and made by the

corresponding author (Figure 1) and adjusting the welding parameters in the automotive robotic line according to Table 1, 20 samples of three-sheet spot-welded joints were fabricated. Figure 2 illustrates a schematic of the joint geometry, including sheet dimensions and the location of spot weld.

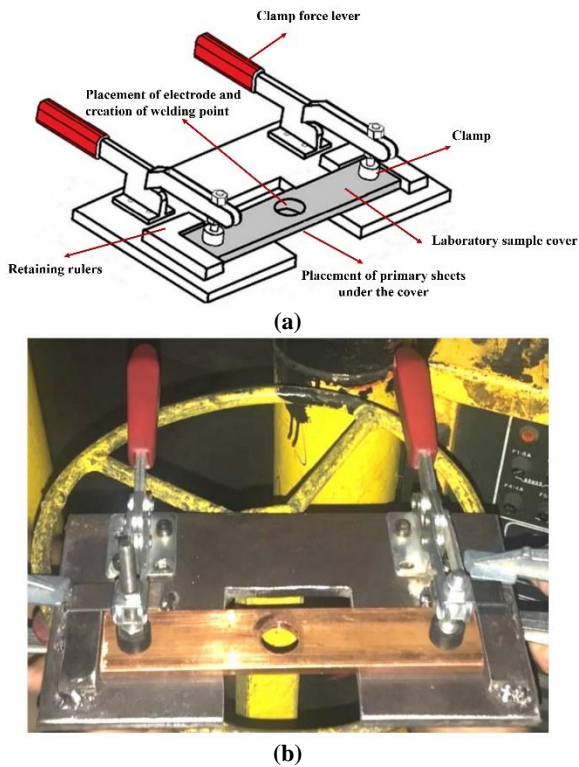


Figure 1. The pre-designed fixture and made by the corresponding author: (a) schematic and (b) real [28]

TABLE 1. Values of the welding process parameters used in the robotic line of the automotive factory to create samples [13]

Parameter	Unit	Value
Force	N	365
Welding current	KA	11.5
Squeeze time	Cycle	25
Upslope	Cycle	3
Welding time	Cycle	12
Hold time	Cycle	9

The fatigue test was performed as axial tension-free loading (positive load ratio and close to zero) with a 10 Hz loading frequency. All the tests were performed as force-controlled constant amplitude loading at room temperature and maintaining stable environmental conditions. These tests were performed at four load levels, including 5000, 4000, 3500 and 3000 N. Also, each test was repeated 5 times and finally the average number of cycles to failure was considered as the fatigue life corresponding to that load level. In the end, with 80 fatigue test results as output parameters along with the applied force and the percentage of the constituent elements of each group as input, the linear regression method was used to find an empirical relationship between them.

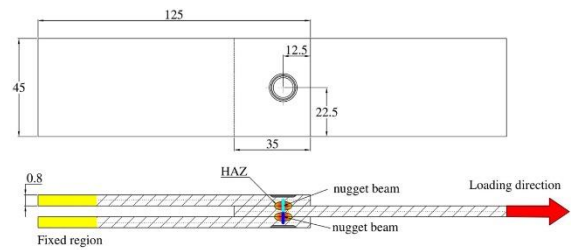


Figure 2. A schematic of the joint geometry, all dimensions are in mm, and boundary conditions in fatigue test [19]

4. RESULTS AND DISCUSSION

The metallographic results for the input sheets indicated that all the sheets are completely ferrite and the grain size in them is equal to grade 7 according to the NFA 04-102 test method (the average grain diameter of 32-37 μm and 900-1000 grains in an area of 1 mm^2 at 100X). Figure 3 shows the microstructure of 1.0347 sheet as a representative. In addition, the results of tensile tests on the test samples according to the ASTM E8M standard at ambient temperature showed that all sheets are within the acceptance range for steel grade 1.0347 (i.e., in the range of 270-370 MPa). Also, this issue was confirmed by the percentage of the constituent elements as the result of the quantitative test. Eventually, the details of the groups considered for future research are reported in Table 2.



Figure 3. Metallographic image of 1.0347 sheet with 100X magnification

TABLE 2. Characteristics of the groups made to continue the research

Case №	Chemical compositions (%)					Static strength (MPa)
	C	Si	Mn	P	S	
1	0.044	0.005	0.184	0.008	0.005	317
	5	5	9	2	3	
2	0.041	0.004	0.183	0.008	0.008	308
	5	5	6	7	2	
3	0.041	0.005	0.183	0.008	0.008	298
	5	5	6	7	2	
4	0.036	0.009	0.180	0.006	0.004	279
	6	8	6	6	4	

Moreover, the fatigue test results for different groups are demonstrated in Figure 4. At first glance, it seems that the results have not changed significantly. But this is not true, so for a better understanding, the average results in the form of the number of cycles to failure in each of the load levels were compared with each other in the form of a bar graph (see Figure 5).

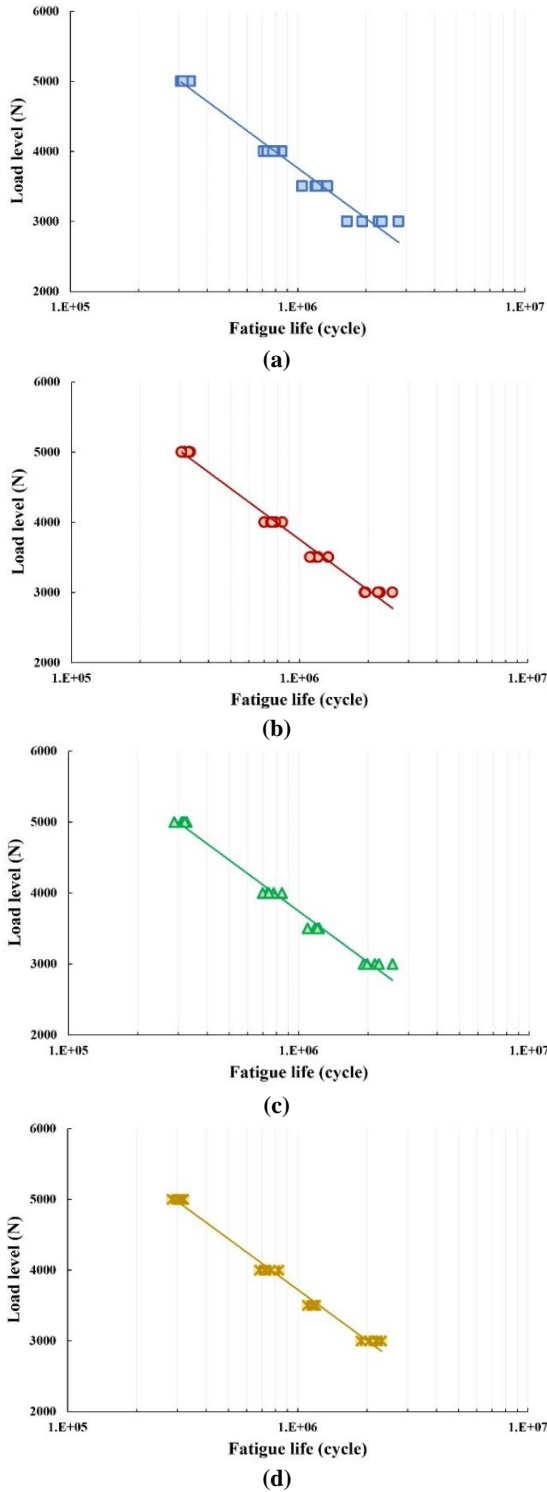


Figure 4. The axial fatigue testing results of the three-sheet spot-welded joints with the same material and sheet thickness in different groups, including: (a) the first group with the sheet tensile strength of 317 MPa, (b) the second group with the sheet tensile strength of 308 MPa, (c) the third group with sheet tensile strength of 298 MPa, and (d) the fourth group with sheet tensile strength of 279 MPa

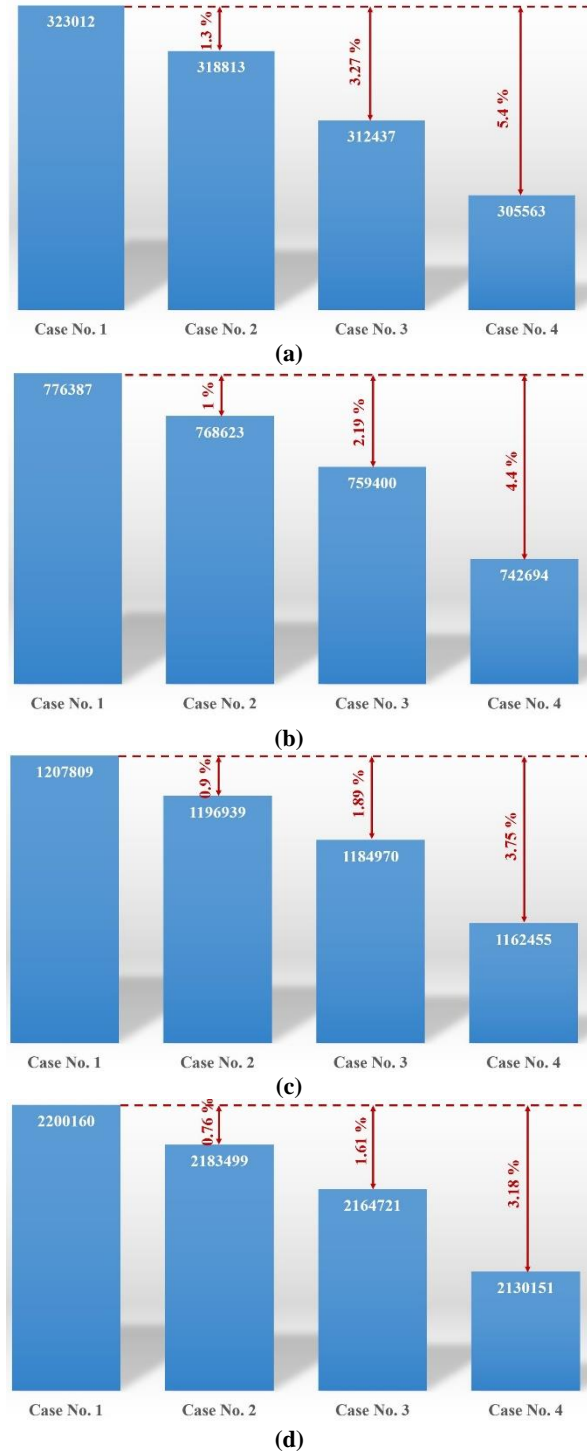


Figure 5. The strength of different samples of three-sheet spot-welded joint under cyclic axial loading, including (a) maximum force of 5000 N, (b) maximum force of 4000 N, (c) maximum force of 3500 N, and (d) maximum force of 3000 N

The results show that the last group has the lowest fatigue life at all load levels. On the other hand, the last group has the lowest strength of the primary sheet. In addition, a regular decreasing trend of the fatigue strength of the three-sheet spot-welded joint is observed from the first group to the last one. Therefore, it can be concluded that by reducing the static strength of the primary sheet, the fatigue life of the spot-welded joint decreases. Also, based on the classification made in Table 2, it can be stated that by assuming the constant percentage of the constituent elements of this steel, the reduction of each of the carbon and magnesium elements leads to a decrease in the fatigue strength of the three-sheet spot-welded joint. In addition, by increasing the amount of silicon (Si), a similar result is achieved. According to the laboratory results depicted in Figure 5, in the studied cases, there is up to about 5.4 % difference in fatigue strength under the range of 3000-5000 N axial loads with a positive loading ratio and close to zero. This dispersion of the results should be added to the inherent dispersion of the fatigue phenomenon. Moreover, it was also shown that by reducing the level of applied force, this dispersion is reduced and the range of percentage changes in the fatigue strength of the three-sheet spot-welded joint is reduced. In other words, the effect of the factor investigated in this research is more evident in the LCF regime. In addition, with the increase in the number of cycles to failure of the three-sheet spot-welded joint, this effect becomes weaker. So that it can be predicted that in a VHCF regime, the effect of this factor has reached the minimum value and can be completely ignored.

Furthermore, the fatigue data at different load levels for material groups of 1, 2, and 4 were used so that the following equation can be derived based on multiple linear regression analysis.

$$\text{Cycles} = \alpha - \beta(\text{Force}) + \gamma(\text{Si}) - \delta(C) + \mu(\text{Force})^2 \quad (3)$$

in which:

$$\begin{aligned} \alpha &= 13552248, \\ \beta &= 5272, \\ \gamma &= 18374702, \\ \delta &= 10617654, \\ \text{and } \mu &= 0.5482. \end{aligned}$$

The analysis showed that in this group of steel, the changes of the other constituent elements had no effect on the fatigue strength of the three-sheet spot-welded joint, or it was negligible, and only the amount of two elements, carbon and silicon, is important. In the following, the above relationship was used to predict the fatigue strength of the third group from the material in Table 2 and to obtain the accuracy of the relationship by comparing it with the laboratory data (Figure 5). Table 3 reports a summary of this achievement. From this table, the maximum error of the empirical relationship between the percentage of elements that make up the primary sheet and the fatigue strength of the three-sheet spot-welded joint, considering the same material and thickness of the sheets in the high cycle area, is less than 13.8 %. Also, by moving towards the more cycles, this error reaches less than 2 %. In addition, it is concluded that in higher cycles, this error value tends to zero. The main reason for this was stated in the

interpretation of the laboratory results that the hypothesis investigated in this paper is most important in the LCF behavior and its importance is minimized in the VHCF regime.

TABLE 3. Evaluation of the accuracy of the empirical relationship proposed to estimate the fatigue strength of the spot-welded joint of three sheets of the same material and with a constant thickness

Load level (N)	Cyclic numbers to failure: Experiment data	Cyclic numbers to failure: Predicted by proposed equation	Prediction accuracy (absolute error)
5000	312437	355554.498	13.8 %
4000	759400	693754.498	8.64 %
3500	1184970	1274004.498	7.51 %
3000	2164721	2128354.498	1.68 %

5. CONCLUSIONS

In the present research, the authors investigated a hypothesis for the first time, that is, the effect of a slight difference in the properties of the primary sheets on the fatigue strength of the three-sheet spot-welded joint. Therefore, this is only a preliminary study that needs further development and more study in the future. Nevertheless, the main achievements of this study are:

- The amount of two elements carbon and silicon in the composition of the elements forming the 1.0437 steel sheet has the greatest effect on the fatigue strength of the three-sheet spot-welded joint.
- The hypothesis investigated in this research should be given the most attention to the LCF behaviour of spot-welded joint (i.e., in conditions where loading leads to plastic deformation in the connection).
- The effect of the hypothesis examined in this study decreases with the increase in the number of fatigue failure cycles, so it can be stated that this idea is completely rejected in the VHCF area.
- The empirical equation between the percentage of elements that form the steel of 1.0347 and the fatigue strength of the spot-welded joints in the investigated range has a maximum error of 13.8 %.

6. ACKNOWLEDGMENT

This paper has been supported by the RUDN University Strategic Academic Leadership Program.

7. CONFLICTS OF INTEREST

The authors declare that they have no known competing financial interests or personal relationships that could have appeared to influence the work reported in this paper.

REFERENCES

1. J. Guo, Solid state welding processes in manufacturing, In Handbook of manufacturing engineering and

- technology (2015) 569-592, https://doi.org/10.1007/978-1-4471-4670-4_55.
2. T.R. Mahmood, Q.M. Doos, A.M. AL-Mukhtar, Failure mechanisms and modeling of spot welded joints in low carbon mild sheets steel and high strength low alloy steel, *Procedia Structural Integrity* 9 (2018) 71–85, <https://doi.org/10.1016/j.prostr.2018.06.013>.
 3. K. Reza Kashyzadeh, G.H. Farrahi, M. Minaei, R. Masajedi, M. Gholamnia, M. Shademani, Numerical study of shunting effect in three-steel sheets resistance spot welding, *International Journal of Engineering* 35(2) (2022) 406-416, <https://doi.org/10.5829/ije.2022.35.02b.17>.
 4. A. Habibzadeh, S.I. Golabi, Prediction of fatigue life of spot welding connections subjected to unidirectional dynamic shear load, *Modares Mechanical Engineering* 14(15) (2015) 361-368, https://doi.org/10.1007/978-1-4471-4670-4_55.
 5. G.H. Farrahi, A. Ahmadi, K.R. Kashyzadeh, S. Azadi, K. Jahani, A comparative study on the fatigue life of the vehicle body spot welds using different numerical techniques: Inertia relief and Modal dynamic analyses, *Frattura ed Integrità Strutturale* 14(52) (2020) 67-81, <https://doi.org/10.3221/IGF-ESIS.52.06>.
 6. K. Reza Kashyzadeh, G.H. Farrahi, A. Ahmadi, M. Minaei, M. Ostad Rahimi, S. Barforoushan, Fatigue life analysis in the residual stress field due to resistance spot welding process considering different sheet thicknesses and dissimilar electrode geometries, *Proceedings of the Institution of Mechanical Engineers, Part L: Journal of Materials: Design and Applications* 237(1) (2023) 33-51, <https://doi.org/10.1177/14644207221101069>.
 7. H. Ueda, H. Fujimoto, S. Kikuchi, T. Okada, M. Fukumoto, K. Okamura, E. Nakayama, M. Yasuyama, Finite element simulation of resistance spot welding process for automotive steel, *Nippon Steel and Sumitomo Metal Technical Report* 119 (2018) 103–114.
 8. B. Sadeghian, A. Taherizadeh, T. Salehi, B. Sadeghi, P. Cavaliere, Simulation and microstructure prediction of resistance spot welding of stainless steel to carbon steel, *Metals* 12(11) (2022) 1898, <https://doi.org/10.3390/met12111898>.
 9. A. Anca, A. Cardona, J. Risso, V.D. Fachinotti, Finite element modeling of welding processes, *Appl. Math. Model.* 35 (2011) 688–707, <http://dx.doi.org/10.1016/j.apm.2010.07.026>.
 10. I. Sattari-Far, M.R. Farahani, Effect of the weld groove shape and pass number on residual stresses in butt-welded pipes, *Int. J. Press. Vessel. Pip.* 86 (2009) 723–731, <https://doi.org/10.1016/j.ijpvp.2009.07.007>.
 11. D. Deng, H. Murakawa, Numerical simulation of temperature field and residual stress in multi-pass welds in stainless steel pipe and comparison with experimental measurements, *Comput. Mater. Sci.* 37 (2006) 269–277, <https://doi.org/10.1016/j.commatsci.2005.07.007>.
 12. V.G. Garcia, I. Mejía, F.R. Calderon, J.A. Benito, J.M. Cabrera, FE thermo-mechanical simulation of welding residual stresses and distortion in Ti-containing TWIP steel through GTAW process, *J. Manuf. Process.* 59 (2020) 801–815, <https://doi.org/10.1016/j.jmapro.2020.09.042>.
 13. G. H. Farrahi, K.R. Kashyzadeh, M. Minaei, A. Sharifpour, S. Riazi, Analysis of resistance spot welding process parameters effect on the weld quality of three-steel sheets used in automotive industry: experimental and finite element simulation, *IJE Transactions A: Basics* 33(1) (2020) 148–157, <https://doi.org/10.5829/IJE.2020.33.01A.17>.
 14. Z. Mikno, Z. Bartnik, Heating of electrodes during spot resistance welding in FEM calculations, *Arch. Civ. Mech. Eng.* 16 (2016) 86–100, <http://dx.doi.org/10.1016/j.acme.2015.09.005>.
 15. Y. Li, Z. Wei, Y. Li, Q. Shen, Z. Lin, Effects of cone angle of truncated electrode on heat and mass transfer in resistance spot welding, *Int. J. Heat Mass Tran.* 65 (2013) 400–408, <http://dx.doi.org/10.1016/j.ijheatmasstransfer.2013.06.012>.
 16. S. Ao, C. Li, Y. Huang, Z. Luo, Determination of residual stress in resistance spot-welded joint by a novel X-ray diffraction, *Measurement* 161 (2020) 107892, <https://doi.org/10.1016/j.measurement.2020.107892>.
 17. X. Wan, Y. Wang, P. Zhang, Numerical simulation on deformation and stress variation in resistance spot welding of dual-phase steel, *Int. J. Adv. Manuf. Technol.* 92 (2017) 2619–2629, <https://doi.org/10.1007/s00170-017-0191-7>.
 18. R. Moharrami, B. Hemmati, Numerical stress analysis in resistance spot-welded nugget due to post-weld shear loading, *J. Manuf. Process.* 27 (2017) 284–290, <https://doi.org/10.1016/j.jmapro.2017.05.007>.
 19. G.H. Farrahi, A. Ahmadi, K.R. Kashyzadeh, Simulation of vehicle body spot weld failures due to fatigue by considering road roughness and vehicle velocity, *Simul. Model. Pract. Theory* 105 (2020) 102168, <https://doi.org/10.1016/j.simpat.2020.102168>.
 20. M. Bayir, E. Yücel, T. Kaya, N. Yıldırım, Spot welding parameter tuning for weld defect prevention in automotive production lines: an ML-based approach, *Information* 14(1) (2023) 50, <https://doi.org/10.3390/info14010050>.
 21. P. Muthu, Optimization of the process parameters of resistance spot welding of AISI 316l sheets using Taguchi method, *Mech. Mech. Eng.* 23 (2019) 64–69, <https://doi.org/10.2478/mme-2019-0009>.
 22. M. Maalouf, Z. Barsoum, Failure strength prediction of aluminum spot-welded joints using kernel ridge regression, *Int. J. Adv. Manuf. Technol.* 91 (2017) 3717–3725, <https://doi.org/10.1007/s00170-017-0070-2>.
 23. S. Chokkalingham, N. Chandrasekhar, M. Vasudevan, Predicting the depth of penetration and weld bead width from the infrared thermal image of the weld pool using artificial neural network modeling, *J. Intell. Manuf.* 23 (2012) 1995–2001, <https://doi.org/10.1007/s10845-011-0526-4>.
 24. Y. Luo, C. Li, H. Xu, Modeling of resistance spot welding process using nonlinear regression analysis and neural network approach on galvanized steel sheet, *Adv. Mat. Res.* 291–294 (2011) 823–828,

- <https://doi.org/10.4028/www.scientific.net/AMR.291-294.823>.
25. P. Kah, J. Martikainen, P. Layus, Methods of evaluating weld quality in modern production (Part 1), *Mechanika*, Proceedings of 16th International Conference, At: Kaunis, Lithuania (2011) 164–169, <https://doi.org/10.13140/2.1.1413.9685>.
 26. P. Kah, J. Martikainen, M. Pirinen, Methods of evaluating weld quality in modern production (Part 2), *Mechanika*, Proceedings of 16th International Conference, At: Kaunis, Lithuania (2011) 170–175, <https://doi.org/10.13140/2.1.2462.5440>.
 27. M. Acebes, R.D. Molina, I. Gauna, N. Thorpe, J.C. Guerro, Development of an automated ultrasonic inspection device for quality control of spot welds, 19th World Conference on Non-Destructive Testing (WCNDT 2016), 13-17 June 2016 in Munich, Germany (WCNDT 2016), 21(7) (2016) 1–8.
 28. N. Amiri, G.H. Farrahi, K.R. Kashyzadeh, M. Chizari, Applications of ultrasonic testing and machine learning methods to predict the static and fatigue behavior of spot-welded joints, *J. Manuf. Process.* 52 (2020) 26–34. <https://doi.org/10.1016/j.jmapro.2020.01.047>.
 29. E. Ghafarallahi, G.H. Farrahi, N. Amiri, Acoustic simulation of ultrasonic testing and neural network used for diameter prediction of three-sheet spot welded joints, *J. Manuf. Process.* 64 (2021) 1507–1516, <https://doi.org/10.1016/j.jmapro.2021.03.012>.
 30. L. Hua, B. Wanga, X. Wanga, X. Hea, S. Guan, In-situ ultrasonic detection of resistance spot welding quality using embedded probe, *J. Mater. Process. Technol.* 267 (2019) 205–214, <https://doi.org/10.1016/j.jmatprotec.2018.12.008>.
 31. A. Moghanizadeh, Evaluation of the physical properties of spot welding using ultrasonic testing, *Int. J. Adv. Manuf. Technol.* 85 (2016) 535–545, <https://doi.org/10.1007/s00170-015-7952-y>.
 32. F. Chen, S. Sun, Z. Ma, G.Q. Tong, X. Huang, Effect of weld nugget size on failure mode and mechanical properties of microscale resistance spot welds on Ti–1Al–1Mn ultrathin foils, *Adv. Mech. Eng.* 10(7) (2018) 1–10, <https://doi.org/10.1177/1687814018785283>.
 33. H. Moshayedi, I. Sattari-Far, Numerical and experimental study of nugget size growth in resistance spot welding of austenitic stainless steels, *J. Mater. Process. Technol.* 212 (2012) 347–354, <https://doi.org/10.1016/j.jmatprotec.2011.09.004>.
 34. Y. Lu, A. Peer, T. Abke, M. Kimchi, W. Zhang, Subcritical heat affected zone softening in hot-stamped boron steel during resistance spot welding, *Mater. Des.* 155 (2018) 170–184, <https://doi.org/10.1016/j.matdes.2018.05.067>.
 35. M. Pouranvari, S.P.H. Marashi, Failure mode transition in AHSS resistance spot welds. Part I. Controlling factors, *Mat. Sci. Eng. A-Struct.* 528(29–30) (2011) 8337–8343, <https://doi.org/10.1016/j.msea.2011.08.017>.